Response Letter

D. Vijay Anand, Sixtus Dakurah and Moo K. Chung

August 23, 2022

We sincerely thank the editor and reviewers for many constructive comments, suggestions and corrections that improved the quality of revision substantially. We addressed every issue very carefully and tried our best to improve the quality and technical correctness of the paper further. The edited parts as well as new material are colored in blue in the main manuscript. To increase the reproducibility and transparency, we also distributed the computer codes in `https://github.com/laplcebeltrami/hodge`.

 # Reviewer 1-1 *The authors tried to establish a new graphic method to investigate the brain connections in fMRI studies. In general, the graphic analysis of fMRI is a relatively new field in fMRI. This work was focusing on mathematic and theory, which may need more explanations and examples for the imaging readers. Especially, the following two parts: First, comparisons to the current methods. The authors should provide comparisons between the graphic method and common fMRI methods in the introduction section. Furthermore, the comparisons between the proposed method and the current graphic method or the common methods in the method and the results sections, so as to present the advantages of the proposed work.*

Following the reviewer's suggestions, we have added a new material comparing the proposed method against existing baseline methods. We also completely revised introduction section reflecting new changes as follows.

Understanding the collective dynamics of brain networks has been a long standing question and continues to remain elusive. Many symptoms of the brain diseases such as schizophrenia, epilepsy, autism, and Alzheimer's disease (AD) have shown possible connections with abnormally high levels of synchrony in neural activity [1]. The mechanisms underlying the emergence of this synchronous behaviour, is often attributed to the higher order interactions that occur at multiple topological scales [2, 3]. The higher order interactions are evidenced across multiple spatial scales in neuroscience such as collective firing of neurons [1], simultaneous activation of multiple brain regions during cognitive tasks [4]. The consideration of higher-order interactions can be highly informative for understanding neuronal synchronisation and co-activation of brain areas at different scales of the network [5].

Over the past several decades, significant progress has been made in understanding the structural and functional behavior of the human brain using functional magnetic resonance images (fMRI). In typical fMRI network studies, the brain is usually modelled as a graph whose nodes are specific brain regions and their connectivity is determined by the strength of dependency between brain regions. Often graph theory based methods have been applied to analyze the brain networks using quantitative measures such as centrality, modularity and small-worldness [6, 7, 8, 9, 10], which allows to interpret and understand the spatial and functional organization of the brain. Besides, graph measures also provide reliable and quantifiable biomarkers that can discriminate normal and clinical populations [11]. Hence, the graph measures are used to identify and quantify the differences in the functional networks at both the individual and group level [6]. The graph comparisons are often performed in the form of either distance-based comparisons or statistics applied theory features [12, 6, 13].

Although graph-based methods can be used to identify graph attributes at disparate scales ranging from local scales at the node level up to global scales at the community level, their power is limited to mostly pairwise dyadic relations [8]. The inherent *dyadic* assumption limits the types of neural structure and function that the graphs can model [14, 15]. Therefore, brain network models built on top of graphs cannot encode higher order interactions, i.e., three- and four-way interactions, beyond pairwise connectivity *without* additional analysis [16]. Despite these limitations the graph-based approaches were often used in brain network analysis [17]. To overcome these limitations, we propose to use topological data analysis (TDA). The TDA has gained a lot of traction in recent years due to its simplistic construct in systematically extracting information from hierarchical layers of abstraction [18]. The algebraic topology in TDA has mathematical ingredients that can effectively manipulate structures with higher order relations. One such tool is the *simplicial complex* which captures many body interactions in complex networks using basic building blocks called simplices [14]. The simplicial complex representation easily encode higher order interactions by the inclusion of 2-simplices (faces) and 3-simplices (volumes) to graphs. We can further adaptively increases the complexity of connectivity hierarchically from simple node-to-node interaction to more complex higher order connectivity patterns easily. Simplicial complexes have been used to represent and analyse the brain data [14, 19, 20]. The modular structure of network can easily be recognized by means of connected components, which is the first topological invariant that characterizes the shape of the network [18]. The cycle on the other hand is a second topological invariant which are loops in the network [21, 22, 23].

The persistent homology (PH), main TDA technique deeply rooted in simplicial complexes, enables network representation at different spatial resolution and provides a coherent framework for obtaining higher order topological features [24, 18]. The PH based approaches are becoming increasingly popular to understand the brain imaging data [21, 25, 13]. The main approach of PH applied to brain networks is to generate a series of nested networks over every possible parameter through a filtration [26]. In particular, the *graph filtration* is the most often used filtration specifically designed to uncover the hierarchical structure of the brain networks in a sequential manner [23].

Topology-based comparison methods infer the similarity and dissimilarity of networks based on PH feature summaries such as persistent diagrams and persistent landscapes [27, 28, 21, 29]. Typically, a topological discriminating function acts on these PH summaries to discern their topological similarity or dissimilarity [27, 28, 21, 24]. The common network distances in the literature for comparing brain networks are the Gromov-Hausdorff (GH) distance and bottleneck (BN) distances [13]. The GH and BN distances are regarded as PH-based distances since they can naturally act on PH feature summaries [24, 13].

In the last two decades, the persistent homology techniques have made significant inroads in neuroimaging analysis particularly for uncovering global topological features beyond pairwise interactions [25]. These global features are the topological invariants such as number of connected components, number of cycles or holes in a network [30, 31]. Traditional persistent homology based methodologies in neuroimaging have mostly focussed on using these topological invariants as biomarkers for identifying and characterising the topological disparities between the control and diseased populations [22, 32]. While the connected structures of the brain network has been extensively investigated, the studies on the cycles in modeling brain networks is very limited [2, 23, 22, 8, 28]. The presence of more cycles in a network signifies a dense connection with stronger connectivity. The cycles in the brain network not only determines the propagation of information but also controls the feedback [33]. Since the information transfer through cycles can occur in two different paths, it is sometimes interpreted as redundant connections. Further, it is also associated with the information diffusion, dissemination, redundancy and information bottleneck problems [34, 35, 36].

While cycles appear naturally in networks, it is not easy to extract or enumerate them. The cycles are often computed using brute-force depth-first search algorithms [37]. Recently, a scalable algorithm for computing the number of cycles in the network was proposed [28]. The cycle or holes is usually identified by manipulating the boundary matrix in the persistent homology [24, 38]. A better approach to determine cycles is by computing the eigenvectors corresponding to zero eigenvalues of Hodge Laplacian [22]. This approach generalizes graph Laplacian (0-Laplacian) applied to nodes (0-simplices) to higher order simplexes [39]. Although these algorithms are useful to extract cycles in small networks, it is computationally not feasible to construct and manipulate higher order simplices and extract cycles for large networks. Ideally, we need algorithms that can capture the essence of higher order interactions and yet retain the simplicity of graph-based approaches.

We propose a new spectral method using the Hodge Laplacian that can explicitly identify the connections associated with the cycles. The method is further capable of localizing the connections contributing to the difference and extract the most discriminative cycles in a network. This is made possible by computing the independent cycle basis and then subsequently building a new statistical inference framework that identifies the most discriminating cycles. To the best of our knowledge there is no efficient algorithm in literature to extract and quantify cycles from brain networks. For the numerical implementation, we propose an efficient new algorithm based on the birth death decomposition of graphs [27].

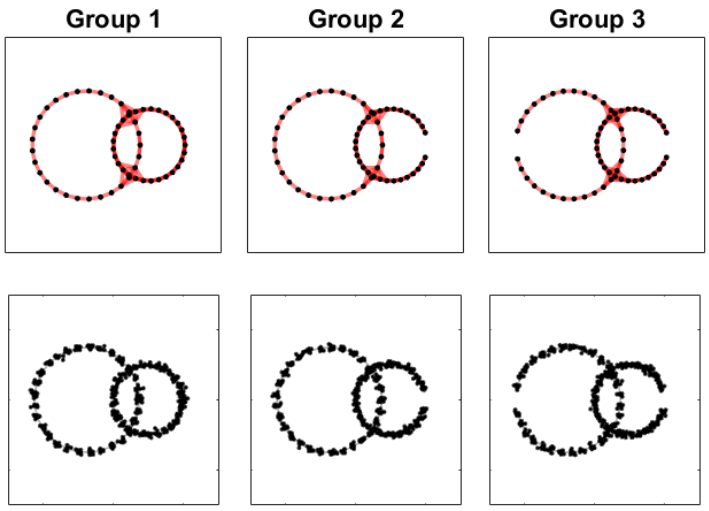

Figure 1: Top: Three topologically different network shapes with different number of loops in each group. Group 1 has three loops, Group 2 has two loops and Group 3 has one loop. Bottom: The sample points for the simulation networks generated using the Gaussian noise $\mathcal{N}(0, 0.05^2)$ on the base network.

We also added an additional validation study as follows.

In literature, there is no baseline method for explicitly modeling cycles in a network. Also, there is no ground truth in real brain data; so even if we apply the baseline methods to real data, it is unclear which method provides the best answer. Thus we first compared our method in a simulation study with the ground truth. To perform a simulations, we construct topologically different shapes by combining circular arcs with and without a gap. The simulation networks are generated by sampling points from different topological shapes as shown in Figure 1. We consider three topologically different networks with the difference in their number of loops in each group. Group 1 has three loops, Group 2 has two loops and Group 3 has one loop. An individual network in each group is generated by first sampling the coordinates y_i along the ground truth patterns. The coordinates of y_i are perturbed with Gaussian noise $\mathcal{N}(0, 0.05^2)$. The weight w_{ij} between any two nodes is given by the Euclidean distance between the coordinates y_i and y_j. To retain only the dominant loops in the network, we applied the following thresholding scheme

$$w'_{ij} = w_{ij}(1 - I_{ij}) + 10^{-3} I_{ij} \cdot U(0, 1),$$

where $U(0, 1)$ is the uniform distribution on the interval $(0, 1)$ and the indicator $I_{ij} = 1$ if $w_{ij} > 0.5$ and 0 otherwise. The edge weights w'_{ij} are constructed such that the connections larger than the threshold 0.5 are replaced with random noise to retain only the dominant loops in the networks. In the simulation, we generated $N = 60$ random networks per group.

We compared our model to graph theory features (Q-modularity, Betweenness) and persistent homology methods (Gromov-Hausdorff distance and bottle neck distances). Table 1 shows the performance results with the average p-values with the standard deviations. The false negative

Table 1: The performance results showing average p-values with the standard deviations. The false positive and false negative rates are shown in the brackets. Smaller error rates are preferred. The graph theory features Q-modularity $\mathfrak{L}_Q$ and betweenness $\mathfrak{L}_{bet}$ are used. The Gromov-Hausdorff $\mathfrak{L}_{GH}$ and bottleneck $\mathfrak{L}_{BN}$ in persistent homology are used. The $\mathfrak{L}_{\mathfrak{w}}$ is the proposed Wasserstein distance on death values. $\mathfrak{L}_{\mathfrak{c}}$ is the proposed test statistic on the cycle basis.

Groups	$\mathfrak{L}_Q$	$\mathfrak{L}_{bet}$	$\mathfrak{L}_{GH}$	$\mathfrak{L}_{BN}$	$\mathfrak{L}_{\mathfrak{w}}$	$\mathfrak{L}_{\mathfrak{c}}$
1 vs. 2	0.4192 ± 0.28 (0.94)	0.5167 ± 0.28 (0.98)	0.4880 ± 0.30 (0.88)	0.4495 ± 0.30 (0.92)	0.0023 ± 0.00 (0.00)	0.0000 ± 0.00 (0.00)
1 vs. 3	0.3521 ± 0.31 (0.76)	0.4673 ± 0.27 (0.98)	0.4903 ± 0.29 (0.94)	0.5419 ± 0.30 (0.98)	0.0000 ± 0.00 (0.00)	0.0000 ± 0.00 (0.00)
2 vs. 3	0.5671 ± 0.28 (0.96)	0.4672 ± 0.30 (0.96)	0.5503 ± 0.29 (0.98)	0.4362 ± 0.29 (1.00)	0.0144 ± 0.03 (0.06)	0.0000 ± 0.00 (0.00)
1 vs. 1	0.5399 ± 0.26 (0.04)	0.5170 ± 0.28 (0.04)	0.4251 ± 0.26 (0.08)	0.4793 ± 0.27 (0.04)	0.5069 ± 0.29 (0.04)	0.4917 ± 0.25 (0.06)
2 vs. 2	0.5487 ± 0.30 (0.02)	0.5291 ± 0.26 (0.02)	0.5153 ± 0.29 (0.04)	0.5031 ± 0.30 (0.04)	0.4524 ± 0.26 (0.04)	0.5164 ± 0.32 (0.14)
3 vs. 3	0.4836 ± 0.30 (0.08)	0.4608 ± 0.26 (0.06)	0.5322 ± 0.25 (0.04)	0.5464 ± 0.33 (0.10)	0.5069 ± 0.32 (0.04)	0.5086 ± 0.31 (0.04)

rates and false positive rates are also indicated within brackets. The $\mathfrak{L}_Q$, $\mathfrak{L}_{bet}$ are based on the Q-modularity and betweenness [11]. The $\mathfrak{L}_{GH}$ and $\mathfrak{L}_{BN}$ are based on the Gromov-Hausdorff [40] and bottleneck distances [41]. The $\mathfrak{L}_{\mathfrak{w}}$ is Wasserstein distance based on death values. $\mathfrak{L}_{\mathfrak{c}}$ is the statistical inference based on the cycle basis. We use the test statistic (**??**) and the statistical significance is determined using the permutation test.

In testing topological differences (first three rows of Table 1), the existing methods did not performing well failing to identify the topological differences. The proposed methods $\mathfrak{L}_{\mathfrak{w}}$ and $\mathfrak{L}_{\mathfrak{c}}$ performed very well and were able to differentiate topological differences. In testing *no* topological difference (last three rows of Table 1), all the methods performed reasonably well and did not report any false positives. In summary, if there are subtle topological differences that are difficult to differentiate, existing methods will likely to fail while the topological method will likely to detect signals.

In Application section, we performed the baseline methods and included the following changes.

We also tested the standard geometric and PH measures on the brain data using the test statistic designed to evaluate most discriminative cycles. We compared the discriminating power of our method against the PH methods Gromov-Hausdorff (GH) and bottleneck (BN) distances in comparing male and female brain networks. The computed p-values are 0.540 and 0.277 respectively and not able to discriminate the networks. Both the GH and BN distances do not perform well in the real data. We also used graph theory features Q-modularity and betweenness measures [11] using the Brain Connectivity Toolbox [11] and obtained p-values of 0.035 and 0.6202 respectively. Among all 4 baseline methods, Even though Q-modularity performed well,

it cannot be used to identify connections that are responsible for the differences and explicitly localize regions that cause significant topological disparity.

 # Reviewer 1-2 *For example, the page 9 third graph mentioned the accuracy of the proposed method. However, it is not clear what is the golden standard to evaluate the accuracy. The proposed method was compared to a k-mean method. However, the fMRI analysis includes detailed preprocessing steps usually. So it will be more convincing to compare the proposed method to a published method or toolbox.*

Following the reviewer's suggestion, we have removed the k-means clustering in the Application section. Instead we compared our method against widely used graph theory features (Q-modularity, betweeness) and persistent homology methods (Gromov-Hausdorff, bottleneck distances). See our response to Reviewer 1-2 above.

 # Reviewer 1-3 *Second, the results require further explanations. For example, the authors mentioned that the figure 8 presented the differences between male and female brain connectivity. Perhaps the author can highlight the different parts in figure 8 and explain its meanings.*

We have updated the figure and added further biological findings to better explain our results. The following new paragraph is added.

Figure 10 (in revised manuscript and Figure 2 in the response letter) shows five most discriminating cycles corresponding to the maximum observed statistics. It can be seen that some brain connections consistently appear in all the five cycles. The five most discriminating 1-cycles include the following brain regions: superior parietal gyrus (Parietal-Sup-L), inferior parietal lobule (Parietal-Inf-L), Precentral gyrus (Precentral-L), Postcentral gyrus (Postcentral-L), the rolandic operculum (Rolandic-Oper-L, Rolandic-Oper-R), the median cingulate and para cingulate gyri (Cingulum-Mid-R, Cingulum-Mid-L) and the Insula. The connectivities between these regions highlight their importance in discriminating males and females. The symmetric connection between the left and right rolandic operculum, superior parietal lobule and the middle cingulate appear in at least 3 most dominating cycles. We can further localize these regions using the frequency of occurrence f_e of the a particular connection (edge) in each cycle given as

$$f_e = \frac{N_e}{N_c},$$

where is the frequency of occurrence, N_e number of cycles in which a particular edge is present and N_c is the total number of most discriminating cycles chosen for analysis. Figure 8 (Bottom right) specifically shows the edges that have $f_e > 0.5$. The edges connecting the regions Parietal-Sup-L, Precentral-L, Postcentral-L and Rolandic-Oper-L appear in all the 5 cycles and has $f_e = 1.0$. There is known sex difference in the parietal region involved in spatial ability, and particularly involved in mental rotation [42]. [43] reported sex differences in the left parietal,

precentral and postcentral regions in a rs-fMRI study, where Kendall's coefficient of concordance (KCC) was used to measure the similarity of the ranked time series of a given voxel to its nearest 26 neighbor voxels [44, 43]. The sex difference is reported in the left rolandic operculum in rs-fMRI study [45]. While all these previous studies are reporting the sex differences at the node level, we are consistently identifying them at the cycle-level within 5 most dominant cycles.

The edges connecting Rolandic-Oper-L, Rolandic-Oper-R and Insula appear in 4 cycles and has $f_e = 0.8$. The edges connecting Parietal-Sup-L and Parietal-Inf-L and the edges connecting Cingulum-Mid-R, Cingulum-Mid-L and Insula-R occur in 3 cycles and has a $f_e = 0.6$. We believe these brain regions can act as discriminating biomarkers for sexual dimorphism studies including Alzheimer's disease which affects disproportionately more women than men [46].

 # Reviewer 1-4 *In addition, the paper would be more smooth, if some of the mathematics can be put in the appendix.*

To easy the burden for researchers new to the topic, we put significant effort in adding more explanations, additional schematic. We have also revised the manuscript in many places to ensure smooth reading. To ease the burden of translating equations to actual computation, we now distributed the computer codes in `https://github.com/laplcebeltrami/hodge`**.**

#Reviewer 2-1 *I do not feel it is yet well written for someone who does not already know a good deal about persistent homology and after all I think this should have higher impact and it should be more available for our friends the scientists who are more so the neurologists and MD-PhD radiologists. Therefore I am strongly suggesting that the authors add a few expository paragraphs in a few locations, the intro, the conclusion and also a few sentences in the abstract, that summarize what it is that is learned using this methodology, what to expect from it and how it is something that cannot be easily learned elsewhere.*

Following the reviewer's suggestion, we added many new expository paragraphs in multiple places. All the changes are marked with blue color. In Introduction section, we have included many expository paragraphs. The introduction is extensively revised. Please see our response to Reviewer 1-1.

Method section has been changed in many places to increase the readability and access of persistent homology concepts to average readers. Figure 3 has been added to explain the basic ideas such as simplicial complex representation, chain complex, 1-cycle and boundary operations. Figure 4 is added to explain the methodology behind the extraction of cycle basis such as birth death decomposition. All changes to the text in this section are marked blue in the revised manuscript.

In Conclusion section, we have replaced the Figure 10 (in revised manuscript)

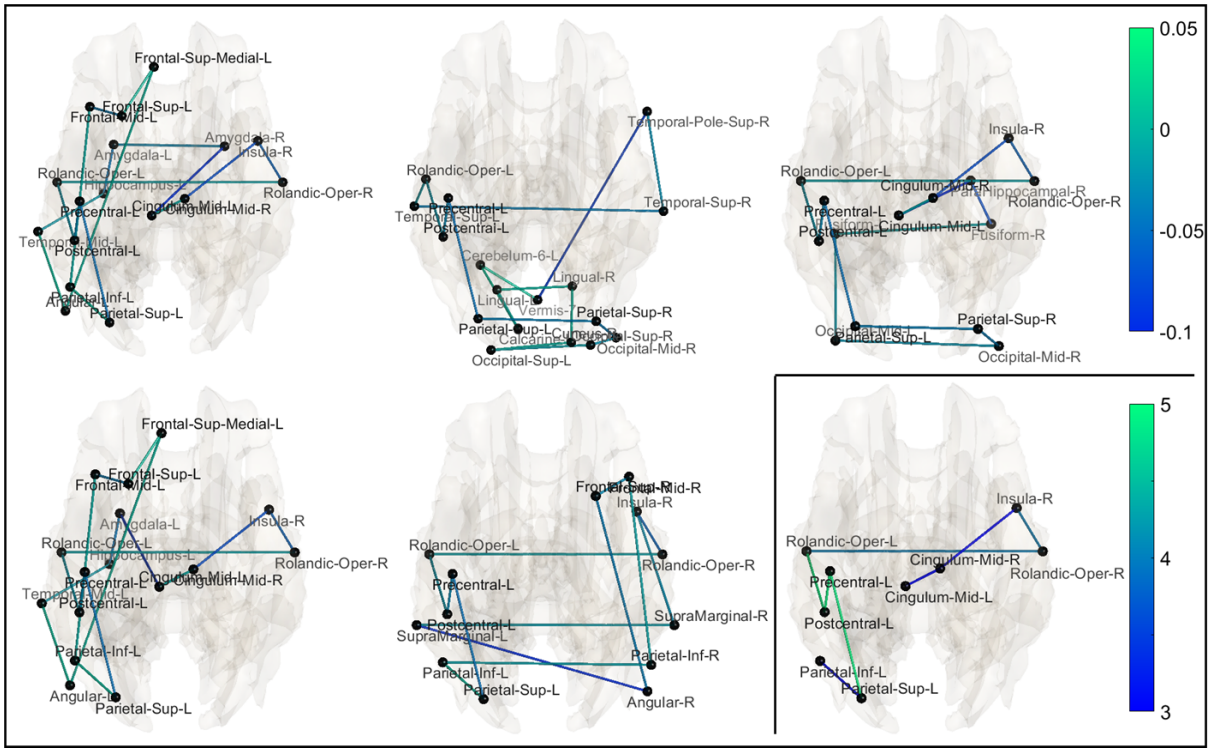

Figure 2: The five most discriminating cycles having the maximum test statistics 0.408, 0.407, 0.405, 0.396 and 0.393 are shown. The color bar in the range -0.10 to 0.05 shows the difference between the average correlation matrices of females and males for the five cycles. Bottom Right: The edges that frequently occur in all the five cycles are shown. The blue edges occur in at least 3 cycles whereas the green edges appear in all the 5 cycles.

with an improved version consisting of 5 most discriminating cycles. Additional explantation for easier biological interpretation has been added. All the changes are marked blue in the revised manuscript.

References

[1] P. J. Uhlhaas and W. Singer, "Neural synchrony in brain disorders: relevance for cognitive dysfunctions and pathophysiology," *Neuron*, vol. 52, no. 1, pp. 155–168, 2006.

[2] H. J. Park and K. Friston, "Structural and functional brain networks: from connections to cognition," *Science*, vol. 342, no. 6158, 2013.

[3] R. F. Betzel and D. S. Bassett, "Multi-scale brain networks," *Neuroimage*, vol. 160, pp. 73–83, 2017.

[4] L. Pessoa, "Understanding brain networks and brain organization," *Physics of Life Reviews*, vol. 11, no. 3, pp. 400–435, 2014.

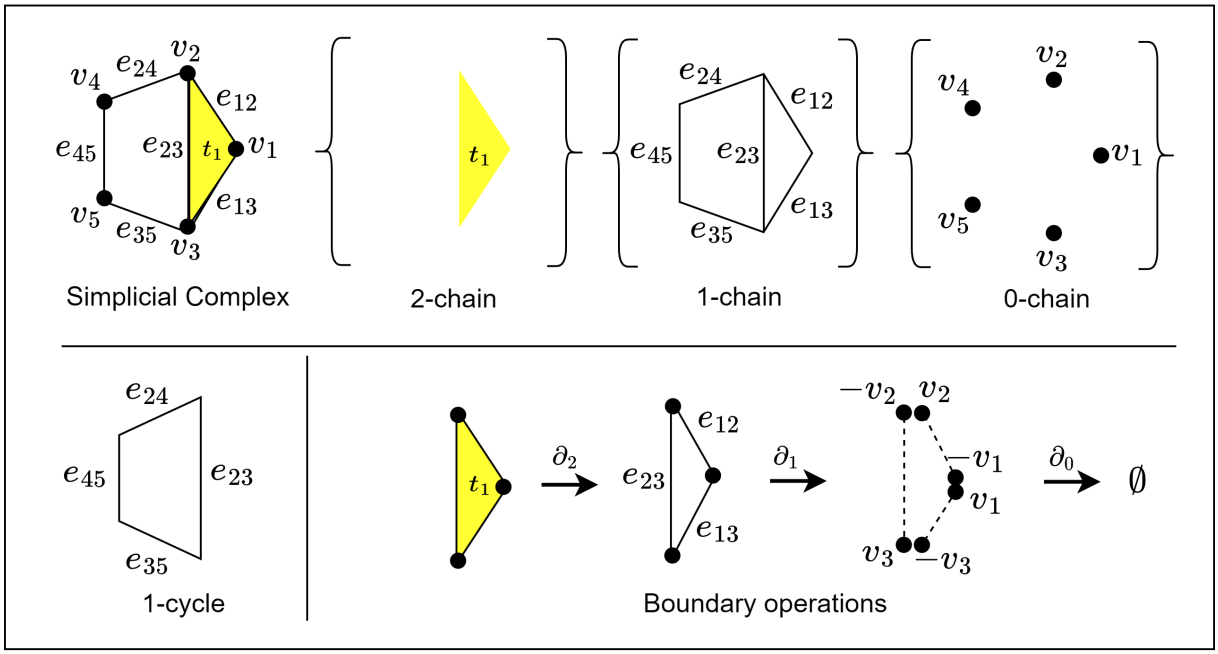

Figure 3: Top left: A simplicial complex with five vertices (0-simplex), six edges (1-simplex) and a triangle (2-simplex colored yellow). The triangle is represented by $t_1 = [v_1, v_2, v_3]$ with a filled-in face (colored yellow). Top left: A chain complex showing 2-chain (set of traingles), 1-chain (set of edges) and 0-chain (set of nodes). Bottom left: The 1-cycle which is present in the simplicial complex. Bottom right: A sequence of boundary operations applied to 2-simplex t_1. After boundary operation ∂_2, we get the 1-simplices $\partial_2 t_1 = [v_1, v_2] + [v_2, v_3] - [v_1, v_3] = e_{12} + e_{23} - e_{13}$, which is the boundary of t_1 [22, 25].

[5] R. Ghorbanchian, J. G. Restrepo, J. J. Torres, and G. Bianconi, "Higher-order simplicial synchronization of coupled topological signals," *Communications Physics*, vol. 4, no. 1, pp. 1–13, 2021.

[6] E. T. Bullmore and O. Sporns, "Complex brain networks: graph theoretical analysis of structural and functional systems," *Nature Reviews Neuroscience*, vol. 10, no. 3, pp. 186–198, 2009.

[7] M. E. Newman, "Finding community structure in networks using the eigenvectors of matrices," *Physical Review E*, vol. 74, no. 3, p. 036104, 2006.

[8] O. Sporns, "Graph theory methods: applications in brain networks," *Dialogues in Clinical Neuroscience*, vol. 20, no. 2, p. 111, 2018.

[9] M. Rubinov and O. Sporns, "Weight-conserving characterization of complex functional brain networks," *Neuroimage*, vol. 56, no. 4, pp. 2068–2079, 2011.

[10] D. S. Bassett and E. T. Bullmore, "Small-world brain networks revisited," *The Neuroscientist*, vol. 23, no. 5, pp. 499–516, 2017.

[11] M. Rubinov and O. Sporns, "Complex network measures of brain connectivity: uses and interpretations," *Neuroimage*, vol. 52, no. 3, pp. 1059–1069, 2010.

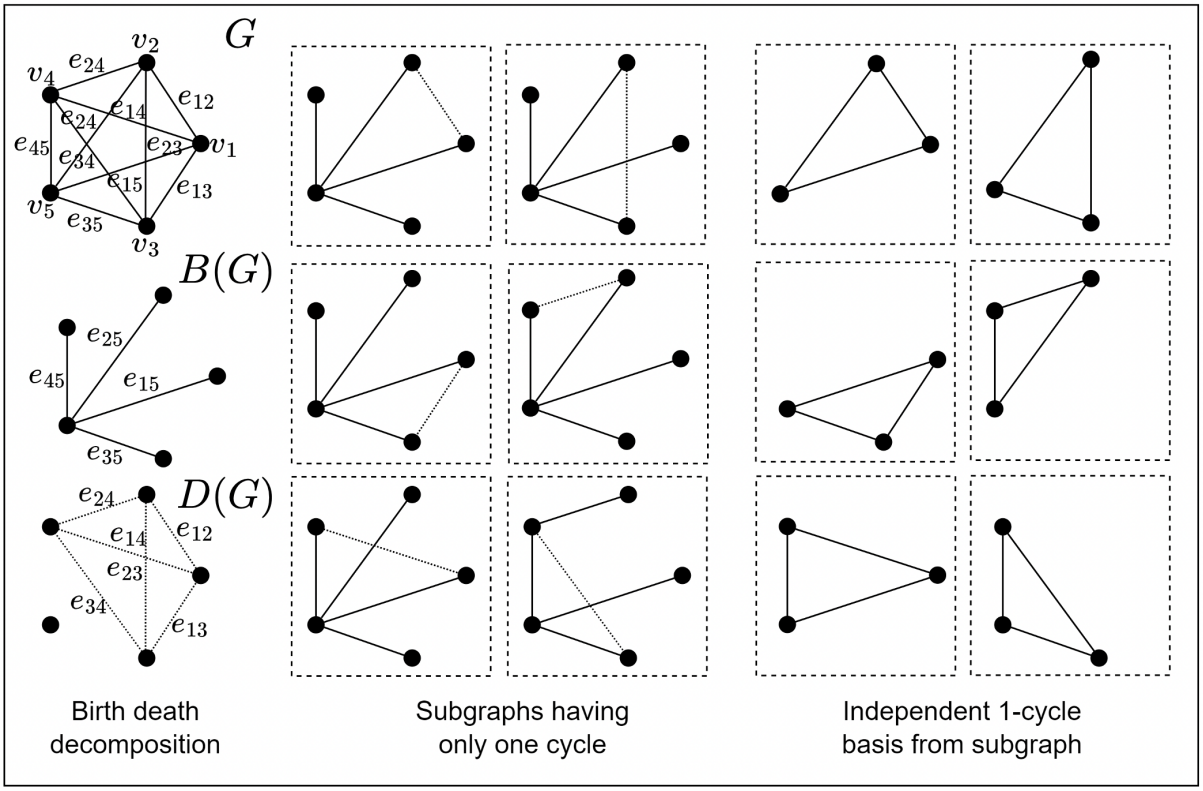

Figure 4: Left: A graph (G) is decomposed into birth set $B(G) = [e_{15}, e_{25}, e_{35}, e_{45}]$ and death set $D(G) = [e_{12}, e_{13}, e_{14}, e_{23}, e_{24}, e_{34}]$. The birth set forms the maximum spanning tree (MST). Middle: The subgraphs constructed by moving an edge from the death set to the birth set (MST). Right: The independent 1-cycles obtained by constructing the Hodge Laplacian on a subgraph and computing its kernel.

[12] A. Mheich, F. Wendling, and M. Hassan, "Brain network similarity: methods and applications," *Network Neuroscience*, vol. 4, no. 3, pp. 507–527, 2020.

[13] M. K. Chung, H. Lee, V. Solo, R. J. Davidson, and S. D. Pollak, "Topological distances between brain networks," in *International Workshop on Connectomics in Neuroimaging*, pp. 161–170, Springer, 2017.

[14] C. Giusti, R. Ghrist, and D. S. Bassett, "Two's company, three (or more) is a simplex," *Journal of Computational Neuroscience*, vol. 41, no. 1, pp. 1–14, 2016.

[15] F. Battiston, G. Cencetti, I. Iacopini, V. Latora, M. Lucas, A. Patania, J.-G. Young, and G. Petri, "Networks beyond pairwise interactions: structure and dynamics," *Physics Reports*, vol. 874, pp. 1–92, 2020.

[16] P. Skardal and A. Arenas, "Higher order interactions in complex networks of phase oscillators promote abrupt synchronization switching," *Communications Physics*, vol. 3, pp. 1–6, 2020.

[17] F. V. Farahani, W. Karwowski, and N. R. Lighthall, "Application of graph theory for identifying connectivity patterns in human brain networks: a systematic review," *frontiers in Neuroscience*, vol. 13, p. 585, 2019.

[18] G. Carlsson, "Topology and data," *Bulletin of the American Mathematical Society*, vol. 46, no. 2, pp. 255–308, 2009.

[19] M. W. Reimann, M. Nolte, M. Scolamiero, K. Turner, R. Perin, G. Chindemi, P. Dłotko, R. Levi, K. Hess, and H. Markram, "Cliques of neurons bound into cavities provide a missing link between structure and function," *Frontiers in Computational Neuroscience*, vol. 11, p. 48, 2017.

[20] G. Petri, P. Expert, F. Turkheimer, R. Carhart Harris, D. Nutt, P. J. Hellyer, and F. Vaccarino, "Homological scaffolds of brain functional networks," *Journal of The Royal Society Interface*, vol. 11, no. 101, p. 20140873, 2014.

[21] M. K. Chung, H. Lee, A. DiChristofano, H. Ombao, and V. Solo, "Exact topological inference of the resting-state brain networks in twins," *Network Neuroscience*, vol. 3, no. 3, pp. 674–694, 2019.

[22] H. Lee, M. K. Chung, H. Kang, and D. S. Lee, "Hole detection in metabolic connectivity of alzheimer's disease using k- laplacian," in *International Conference on Medical Image Computing and Computer-Assisted Intervention*, pp. 297–304, Springer, 2014.

[23] H. Lee, M. K. Chung, H. Kang, B.-N. Kim, and D. S. Lee, "Computing the shape of brain networks using graph filtration and Gromov-Hausdorff metric," in *International Conference on Medical Image Computing and Computer-Assisted Intervention*, pp. 302–309, Springer, 2011.

[24] H. Edelsbrunner, J. Harer, *et al.*, "Persistent homology-a survey," *Contemporary Mathematics*, vol. 453, pp. 257–282, 2008.

[25] A. E. Sizemore, J. E. Phillips Cremins, R. Ghrist, and D. S. Bassett, "The importance of the whole: topological data analysis for the network neuroscientist," *Network Neuroscience*, vol. 3, no. 3, pp. 656–673, 2019.

[26] G. Petri, M. Scolamiero, I. Donato, and F. Vaccarino, "Topological strata of weighted complex networks," *PloS One*, vol. 8, no. 6, p. e66506, 2013.

[27] T. Songdechakraiwut and M. K. Chung, "Topological learning for brain networks," *arXiv preprint arXiv:2012.00675*, 2020.

[28] M. K. Chung, S. G. Huang, A. Gritsenko, L. Shen, and H. Lee, "Statistical inference on the number of cycles in brain networks," in *2019 IEEE 16th International Symposium on Biomedical Imaging (ISBI 2019)*, pp. 113–116, IEEE, 2019.

[29] L. Wasserman, "Topological data analysis," *arXiv preprint arXiv:1609.08227*, 2016.

[30] H. Lee, H. Kang, M. K. Chung, B.-N. Kim, and D. S. Lee, "Persistent brain network homology from the perspective of dendrogram," *IEEE transactions on medical imaging*, vol. 31, no. 12, pp. 2267–2277, 2012.

[31] H. Lee, M. K. Chung, H. Kang, H. Choi, Y. K. Kim, and D. S. Lee, "Abnormal hole detection in brain connectivity by kernel density of persistence diagram and Hodge Laplacian," in *2018 IEEE 15th International Symposium on Biomedical Imaging (ISBI 2018)*, pp. 20–23, IEEE, 2018.

[32] M. Chung, J. Hanson, J. Ye, R. Davidson, and S. Pollak, "Persistent homology in sparse regression and its application to brain morphometry," *IEEE Transactions on Medical Imaging*, vol. 34, pp. 1928–1939, 2015.

[33] P. G. Lind, M. C. Gonzalez, and H. J. Herrmann, "Cycles and clustering in bipartite networks," *Physical Review E*, vol. 72, no. 5, p. 056127, 2005.

[34] H. Lee, K. H. Chung, M.K., and D. Lee, "Hole detection in metabolic connectivity of Alzheimer's disease using k-Laplacian," in *International Conference on Medical Image Computing and Computer-Assisted Intervention (MICCAI), Lecture Notes in Computer Science*, pp. 297–304, 2014.

[35] A. Sizemore, C. Giusti, A. Kahn, J. Vettel, R. Betzel, and D. Bassett, "Cliques and cavities in the human connectome," *Journal of computational neuroscience*, vol. 44, pp. 115–145, 2018.

[36] M. Chung, S.-G. Huang, A. Gritsenko, L. Shen, and H. Lee, "Statistical inference on the number of cycles in brain networks," in *2019 IEEE 16th International Symposium on Biomedical Imaging (ISBI 2019)*, pp. 113–116, IEEE, 2019.

[37] R. Tarjan, "Depth-first search and linear graph algorithms," *SIAM Journal on Computing*, vol. 1, no. 2, pp. 146–160, 1972.

[38] C. Chen and D. Freedman, "Measuring and computing natural generators for homology groups," *Computational Geometry*, vol. 43, no. 2, pp. 169–181, 2010.

[39] F. R. Chung and F. C. Graham, *Spectral graph theory.* No. 92, American Mathematical Society., 1997.

[40] H. Lee, M. Chung, H. Kang, B.-N. Kim, and D. Lee, "Computing the shape of brain networks using graph filtration and Gromov-Hausdorff metric," *MICCAI, Lecture Notes in Computer Science*, vol. 6892, pp. 302–309, 2011.

[41] M. Chung, H. Lee, A. Gritsenko, A. DiChristofano, D. Pluta, H. Ombao, and V. Solo, "Topological brain network distances," *arXiv preprint arXiv:1809.03878*, 2018.

[42] T. Koscik, D. O'Leary, D. Moser, N. Andreasen, and P. Nopoulos, "Sex differences in parietal lobe morphology: relationship to mental rotation performance," *Brain and cognition*, vol. 69, pp. 451–459, 2009.

[43] C. Xu, C. Li, H. Wu, Y. Wu, S. Hu, Y. Zhu, W. Zhang, L. Wang, S. Zhu, and J. Liu, "Gender differences in cerebral regional homogeneity of adult healthy volunteers: a resting-state fMRI study," *BioMed Research International*, vol. 2015, p. 183074, 2015.

[44] Y. Zang, T. Jiang, Y. Lu, Y. He, and L. Tian, "Regional homogeneity approach to fmri data analysis," *Neuroimage*, vol. 22, pp. 394–400, 2004.

[45] L. Rubin, L. Yao, S. Keedy, J. Reilly, J. Bishop, C. Carter, H. Pournajafi-Nazarloo, L. Drogos, C. Tamminga, and G. Pearlson, "Sex differences in associations of arginine vasopressin and oxytocin with resting-state functional brain connectivity," *Journal of neuroscience research*, vol. 95, pp. 576–586, 2017.

[46] D. Fisher, D. Bennett, and H. Dong, "Sexual dimorphism in predisposition to Alzheimer's disease," *Neurobiology of aging*, vol. 70, pp. 308–324, 2018.